JOURNAL OF MATERIALS SCIENCE **36** (2001) 1727–1733

Effect of La and K on the microstructure and dielectric properties of $Bi_{0.5}Na_{0.5}TiO_3$-$PbTiO_3$

S. KUHARUANGRONG
Department of Materials Science, Faculty of Science, Chulalongkorn University, Bangkok 10330, Thailand
E-mail: sutin@sc.chula.ac.th

Small amounts of lanthanum and potassium dopants could modify the microstructure and dielectric properties of $0.90Bi_{0.5}Na_{0.5}TiO_3$-$0.10PbTiO_3$ and $0.88Bi_{0.5}Na_{0.5}TiO_3$-$0.12PbTiO_3$ solid solutions. La lowered both phase transition temperatures of ferroelectric to antiferroelectric and antiferroelectric to paraelectric. It also decreased the maximum value of relative dielectric permittivity of the composition. In contrast, K shifted the first phase transition to the lower temperature but insignificantly affected the Curie temperature and raised the maximum dielectric permittivity. Furthermore, K influenced the microstructure in the way to enhance the long grains of this solid solution but La inhibited this effect.

1. Introduction

$Bi_{0.5}Na_{0.5}TiO_3$ is a ferroelectric [1] at room temperature and has the perovskite structure with a general formula ABO_3, where Bi and Na occupy in the A site. It has a rhombohedral phase [2], $R3m$ [3] with $a = 3.891 \pm 0.002$ angstroms and $\alpha = 89°36' \pm 3'$. Above the first transition temperature which is about 220°C [4] it changes to an antiferroelectric [5]. At 320°C there is a transition to the paraelectric tetragonal phase and it changes to the paraelectric cubic phase at 520°C. This material was considered to be a good candidate for lead-free piezoelectric and pyroelectric devices. Thus, most studies concentrated on the piezoelectric [6–10] and pyroelectric [6–7, 11–12] properties of $Bi_{0.5}Na_{0.5}TiO_3$ and its modifications. Although many investigations try to develop lead-free materials to avoid the evaporation of PbO and its pollution, lead-based $Bi_{0.5}Na_{0.5}TiO_3$ gives much more excellent properties. $Bi_{0.5}Na_{0.5}TiO_3$ doped with 6.5%Sr and 6.5%Pb was found to be suitable for ultrasonic transducers at high frequency with a low permittivity and a high electromechanical coupling factor [9]. With 5%Sr and 5%Pb, this composition was considered to be useful for pyroelectric sensors [8] with a large figure of merit and comparable to $Pb(Zr,Ti)O_3$. Nevertheless, the modifications of $Bi_{0.5}Na_{0.5}TiO_3$ and Pb-based this system for a high temperature dielectric have not been widely investigated. Previous study [13] showed that the morphotropic phase boundary of $Bi_{0.5}Na_{0.5}TiO_3$-$PbTiO_3$ was found between 15–17%Pb, since the structure changed from rhombohedral to tetragonal, resulting in loss of a relaxor characteristic. Thus, 15%Pb-doped-$Bi_{0.5}Na_{0.5}TiO_3$ is not suitable to modify for a stable high temperature dielectric. 10%Pb- and 12%Pb-doped $Bi_{0.5}Na_{0.5}TiO_3$ are selected as base materials for this study. Sr and Ba dopants can increase the maximum dielectric permittivity of $0.90Bi_{0.5}Na_{0.5}TiO_3$-$0.10PbTiO_3$ but decrease its Curie temperature [5, 14]. In this work the effects of La and K on the microstructure, dielectric properties and transition temperatures of these two solid solutions are presented.

2. Experiment

2.1. Sample preparation

The compositions selected for this investigation were as follows:

$0.88(Bi_{0.5}Na_{0.5}TiO_3)$-$0.12PbTiO_3$ or 12%Pb-doped-$Bi_{0.5}Na_{0.5}TiO_3$

$0.88(Bi_{0.48}La_{0.02}Na_{0.5}TiO_3)$-$0.12PbTiO_3$ or B48L2P12

$0.88(Bi_{0.45}La_{0.05}Na_{0.5}TiO_3)$-$0.12PbTiO_3$ or B45L5P12

$0.88(Bi_{0.48}La_{0.02}Na_{0.45}K_{0.05}TiO_3)$-$0.12PbTiO_3$ or B48L2K5P12

$0.90(Bi_{0.45}La_{0.05}Na_{0.5}TiO_3)$-$0.10PbTiO_3$ or B45L5P10

$0.90(Bi_{0.45}La_{0.05}Na_{0.45}K_{0.05}TiO_3)$-$0.10PbTiO_3$ or B45L5K5P10

In this notation, all cations on the A-site except Na are denoted. In maintaining the proportion, however, the total number of Na and K is equal to 0.5. All above compositions were prepared by mixing and calcining all oxides and carbonates. Reagent grade of Bi_2O_3, Na_2CO_3,

TiO_2, PbO, La_2O_3 and K_2CO_3 were used as the starting raw materials. They were weighed and mixed by ball milling in a high density polyetylene bottle using zirconia rods and ethanol. After drying, the mixture was calcined in oxygen with a heating rate of 2°C/min, and held at the reaction temperatures determined from the differential thermal analysis (DTA). The data were taken with a heating rate of 10°C/min in oxygen.

After calcining, the powder was taken to characterize a phase by X-ray diffraction (XRD) using Cu K_α radiation.

The calcined material was remilled and polyvinyl alcohol was added as a binder. After drying, the grinded powder was pressed into disks on a single action drypress and followed by cold-isostatic press. After binder burnout, the pressed disks were sintered at 1175°C with an hour soaking at this temperature in a closed crucible.

2.2. Characterization

The microstructure of the sintered samples was observed by scanning electron microscopy (SEM). All samples were polished and thermally etched at 1075°C.

The diameter and thickness of disks were measured for the calculation of the relative dielectric permittivity. The disks were electroded with fired-on silver paste. All capacitance and dissipation factor measurements were obtained from HP4192A Impedance Analyzer using a four-terminal configuration. All data were collected at different frequencies and every 3°C with increasing temperature at 3°C/min from room temperature.

3. Results and discussion

The differential thermal analysis of the milled raw materials for the compositions of B48L2P12, B48L2K5P12, B45L5P10 and B45L5K5P10 is shown in Fig. 1. The data indicate that the reactions complete before 750°C due to no additional peaks observed above this temperature. The results from DTA measurement imply that the suitable calcination temperature for all these compositions should be 750°C. Nevertheless, the weight loss during calcination is higher than that

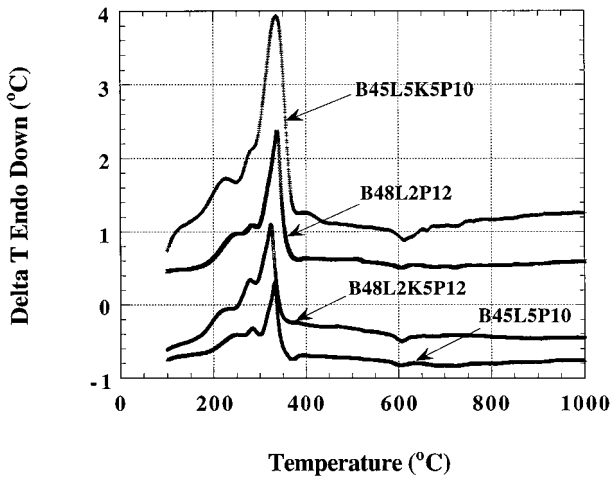

Figure 1 DTA curves of B48L2P12, B48L2K5P12, B45L5P10 and B45L5K5P10.

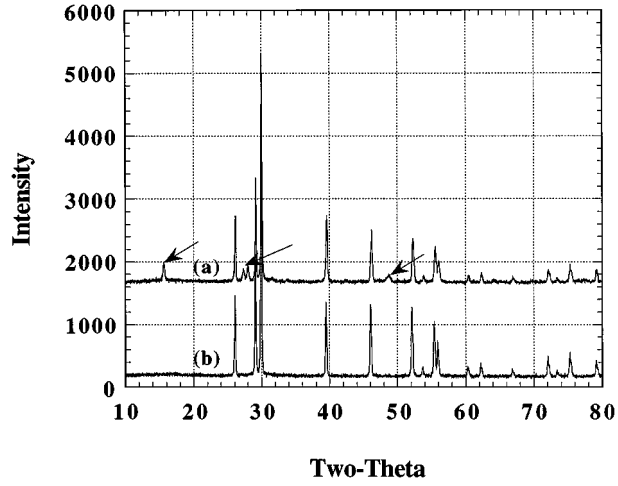

Figure 2 XRD patterns at room temperature of lanthanum oxide (a) before and (b) after calcination at 1000°C.

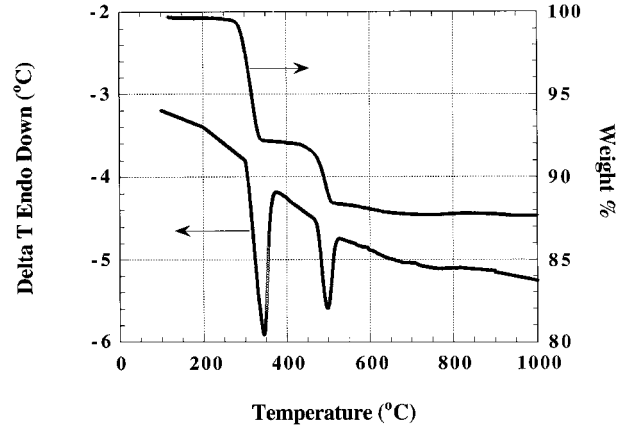

Figure 3 DTA and TGA curves of lanthanum oxide as a starting material.

calculated from oxides and carbonates as starting raw materials.

Fig. 2 reveals the x-ray patterns at room temperature for lanthanum oxide (from J.T Baker and Aldrich) as a starting material before and after calcination at 1000°C. The small diffraction peaks of two-theta at 15.6, 27.3, 28.0 and 48.7 of $La(OH)_3$ are observed in lanthanum oxide and disappeared after calcination. This is confirmed by the result from DTA. The two endothermic reactions occur around 340°C and 480°C as illustrated in the Fig. 3. The weight loss of this raw material was also determined by thermogravimetric analysis (TGA) with a heating rate of 10°C/min. Two temperature intervals of the decomposition reactions are detected, corresponding to the result from DTA. This is possibly attributed to water removal from $La(OH)_3$. The total weight loss is 12% in this observation. In addition, the ratio of weight loss between these two temperatures is 2 : 1, suggesting that two molecules of water lost during the first reaction step and the other one removed in the last temperature interval. As a consequence, lanthanum oxide was calcined at 1000°C before weighing and mixing with other raw materials.

Fig. 4 shows the x-ray patterns at room temperature for the calcined powder of B48L2P12, B45L5P10, B48L2K5P12 and B45L5K5P10. The patterns of B48L2P12 and B45L5P10 exhibit the same

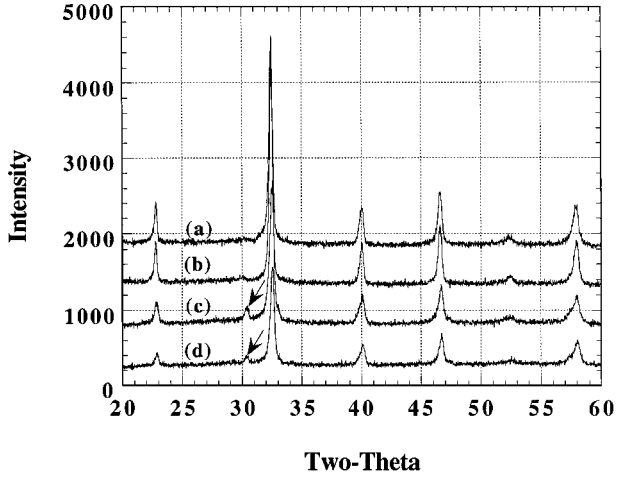

Figure 4 XRD patterns at room temperature of (a) B48L2P12, (b) B45L5P10, (c) B48L2K5P12 and (d) B45L5K5P10.

phase and structure as obtained in $Bi_{0.5}Na_{0.5}TiO_3$ and $0.90Bi_{0.5}Na_{0.5}TiO_3$-$0.10PbTiO_3$ [13]. The results of DTA and XRD imply that the formation of perovskite of these two compositions can complete at 750°C. However, a small peak of two-theta at 30.3 is detected in the patterns of K-doped into these compositions. This suggests that the addition of K forms a second phase or an intermediate phase of these solid solutions. In spite of calcination at higher temperature, 850°C, this small reflection still exists in the XRD investigation.

SEM photomicrograph of 12%Pb-doped-$Bi_{0.5}Na_{0.5}TiO_3$ sintered at 1175°C is revealed in Fig. 5. Some long grains are present in the thermally etched surface of this composition. An addition of a small amount of La contributes to the smaller grain size and reduces the number of elongated grains in this composition as illustrated in Fig. 6. Moreover, the increasing amount

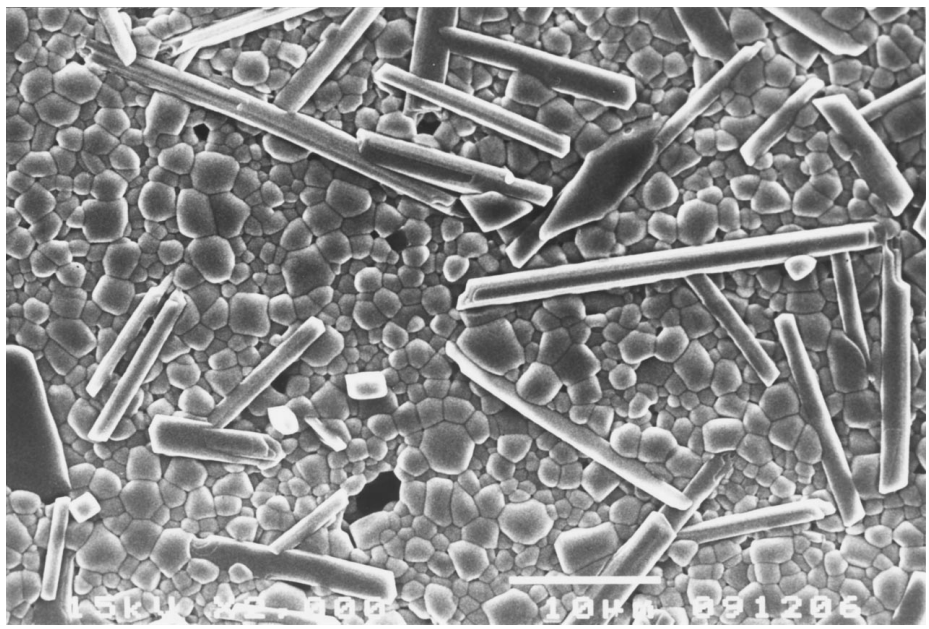

Figure 5 SEM micrograph of 12%Pb-doped $Bi_{0.5}Na_{0.5}TiO_3$.

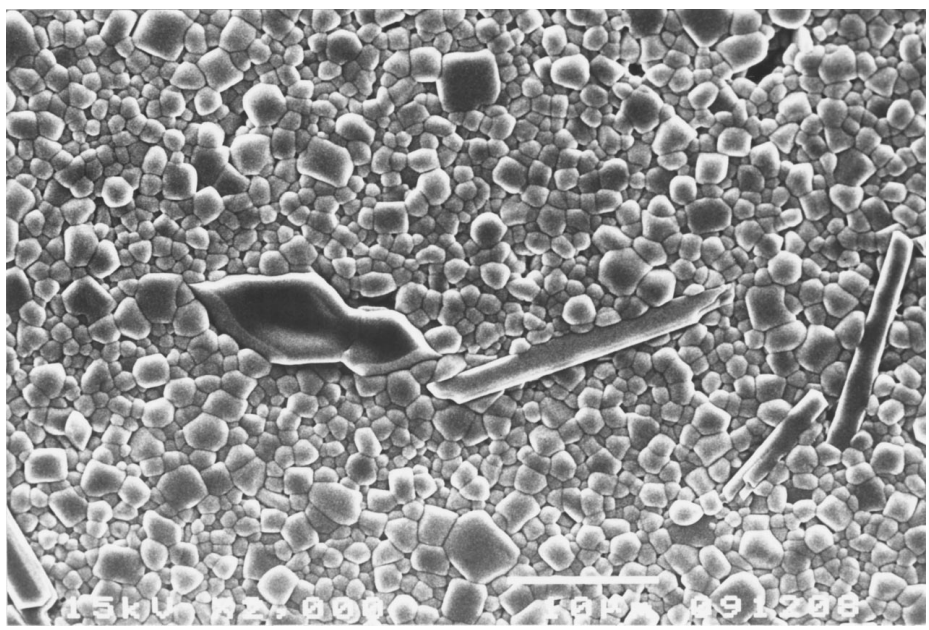

Figure 6 SEM micrograph of $0.88(Bi_{0.48}La_{0.02}Na_{0.5}TiO_3)$-$0.12PbTiO_3$.

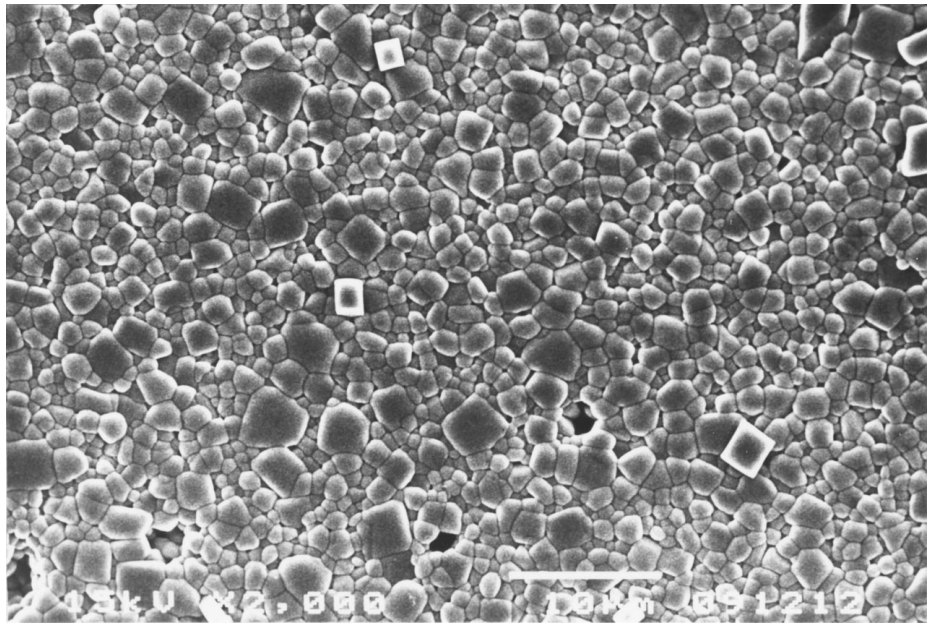

Figure 7 SEM micrograph of $0.88(Bi_{0.45}La_{0.05}Na_{0.5}TiO_3)$-$0.12PbTiO_3$.

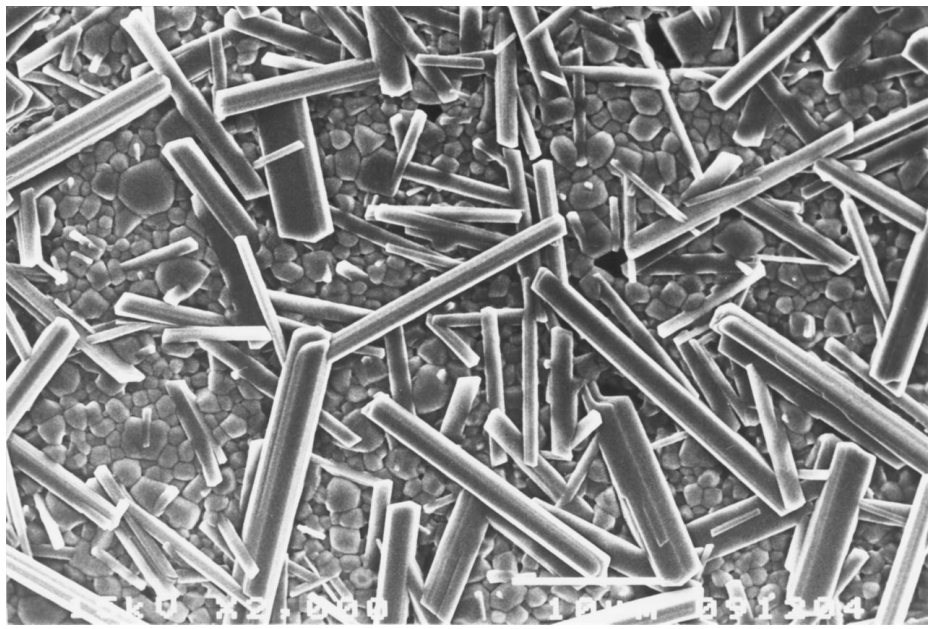

Figure 8 SEM micrograph of $0.88(Bi_{0.48}La_{0.02}Na_{0.45}K_{0.05}TiO_3)$-$0.12PbTiO_3$.

of La can enhance this performance (Fig. 7). On the contrary, K dopant increases the number of elongated grains in $0.88(Bi_{0.48}La_{0.02}Na_{0.5}TiO_3)$-$0.12PbTiO_3$ as given in Fig. 8. These results indicate that Pb and K promote the long grains of $Bi_{0.5}Na_{0.5}TiO_3$ but La prevents this effect. The detection of long grains is also dependent upon the sintering temperature. This was observed in the SEM micrographs of $0.83Bi_{0.5}Na_{0.5}TiO_3$-$0.17PbTiO_3$ sintered at 1200°C but not 1175°C in the previous work [13]. Although Pb enhances the long grains, with decreasing Pb there is a tendency of grain growth, which can be seen in the microstructures of B45L5P12 (Fig. 7) and B45L5P10 (Fig. 9). Unexpectedly, doping with K is effective in suppressing the long grains and grain growth of B45L5P10 as appeared in Fig. 10. It should also be mentioned here that a few of long grains can be perceived in some area of this polished composition. From these results the shape and size of grains of $Bi_{0.5}Na_{0.5}TiO_3$-$PbTiO_3$ strongly depend on the sintering temperature, the dopant and its amount. Additionally, a second phase is imperceptible in the micrograph of B45L5K5P10 (Fig. 10). As compared to the XRD result of this material in which a small peak of the second phase or intermediate phase appears, these demonstrate that this phase significantly reduces after sintering at 1175°C.

The result of the relative dielectric permittivity as a function of temperature and frequency of 12%Pb-doped-$Bi_{0.5}Na_{0.5}TiO_3$ is shown in Fig. 11. The first phase transition temperature at which the ferroelectric starts transforming to antiferroelectric in this composition occurs around 125°C. Apparently, 12%Pb can

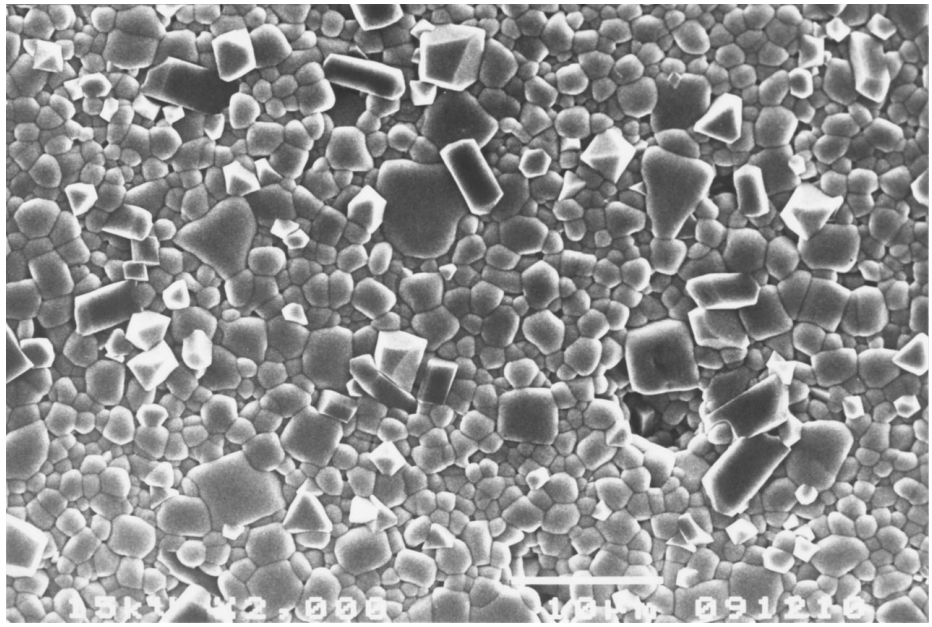

Figure 9 SEM micrograph of $0.90(Bi_{0.45}La_{0.05}Na_{0.5}TiO_3)$-$0.10PbTiO_3$.

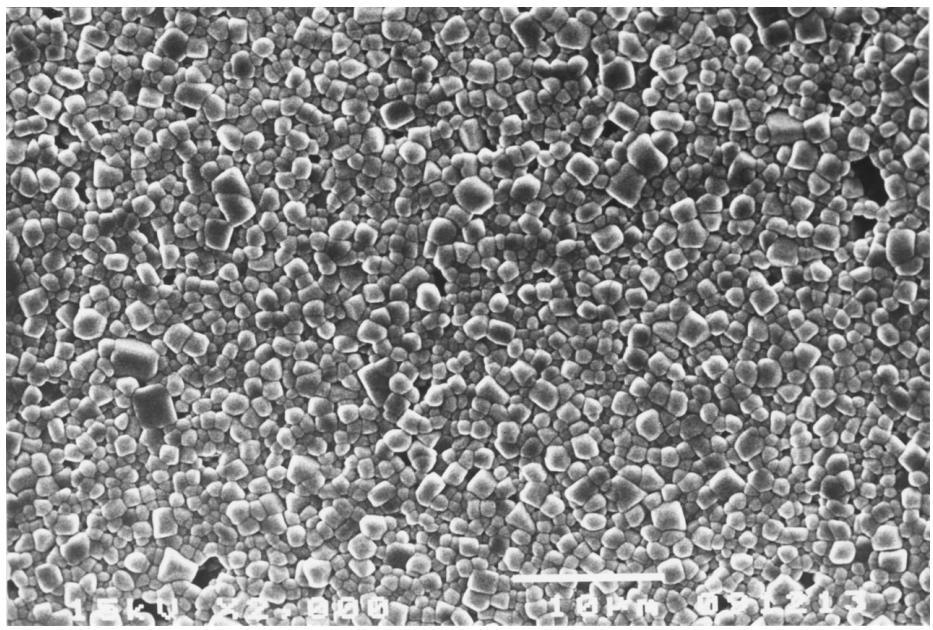

Figure 10 SEM micrograph of $0.90(Bi_{0.45}La_{0.05}Na_{0.45}K_{0.05}TiO_3)$-$0.10PbTiO_3$.

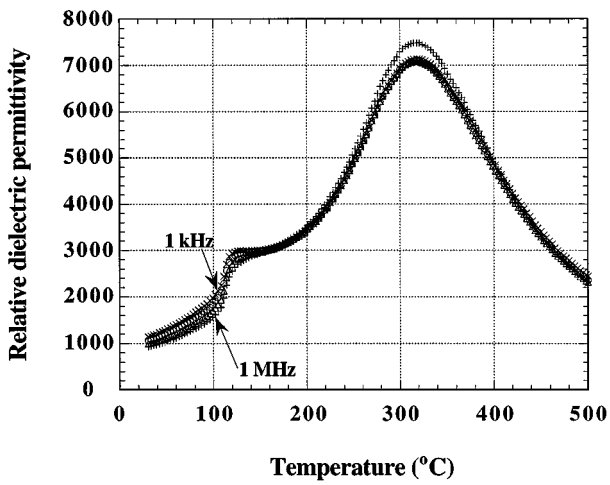

Figure 11 Change in the relative dielectric permittivity with temperature and frequency for 12%Pb-doped $Bi_{0.5}Na_{0.5}TiO_3$.

lower this transition of $Bi_{0.5}Na_{0.5}TiO_3$ from 220°C [4–5, 13] and $0.90Bi_{0.5}Na_{0.5}TiO_3$-$0.10PbTiO_3$ from 140°C [13]. In addition, it increases the dielectric permittivity at 10 kHz of $Bi_{0.5}Na_{0.5}TiO_3$ [13] from 700 to 1400 and 2640 to 7100 at room temperature and the Curie point, respectively. With the addition of La, not only the ferroelectric to antiferroelectric but the antiferroelectric to paraelectric phase transitions of 12%Pb-doped-$Bi_{0.5}Na_{0.5}TiO_3$ shift toward lower temperatures which can be seen in Fig. 12. The result also shows the decreasing maximum dielectric permittivity at 10 kHz of La-doped in this composition from 7100 to 5400 at the Curie temperature. In Fig. 13 the first transition of B48L2P12 can be further extended to lower temperature with K dopant. Moreover, K not only raises the relative dielectric permittivity at room temperature and the Curie point but displays a strong relaxor characteristic

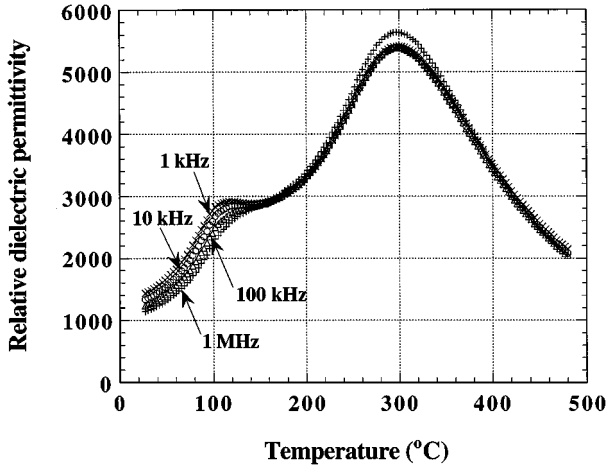

Figure 12 Change in the relative dielectric permittivity with temperature and frequency for 0.88($Bi_{0.48}La_{0.02}Na_{0.5}TiO_3$)-0.12$PbTiO_3$.

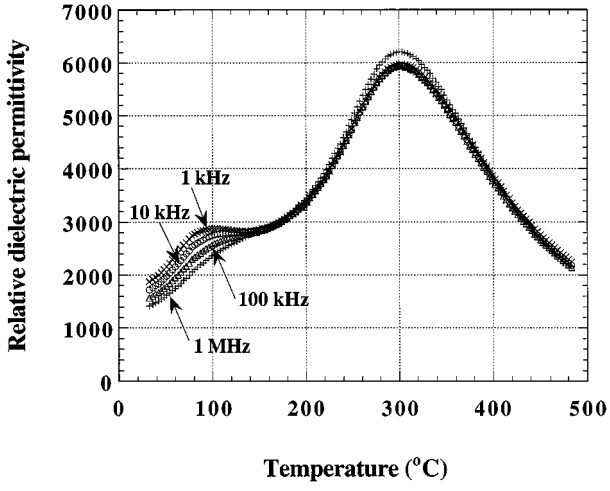

Figure 13 Change in the relative dielectric permittivity with temperature and frequency for 0.88($Bi_{0.48}La_{0.02}Na_{0.45}K_{0.05}TiO_3$)-0.12$PbTiO_3$.

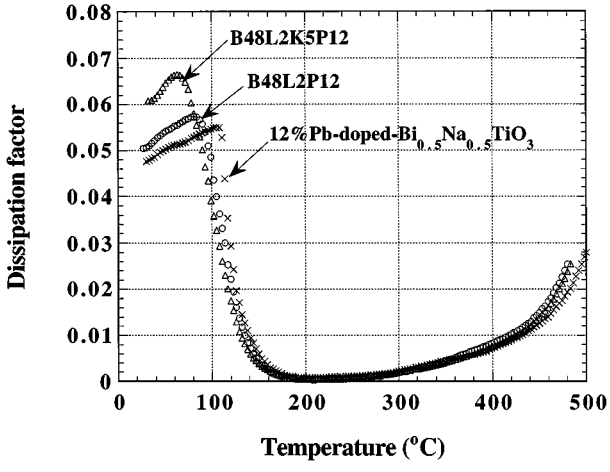

Figure 14 Change in the dissipation factor with temperature at 10 kHz for 12%Pb-doped $Bi_{0.5}Na_{0.5}TiO_3$, B48L2P12 and B48L2K5P12.

in which the dielectric permittivity is dependent upon the measuring frequency and the transition temperature at higher measuring frequency displaces to higher temperature. Fig. 14 illustrates the results of the dissipation factor as a function of temperature at a frequency of 10 kHz of 12%Pb-doped-$Bi_{0.5}Na_{0.5}TiO_3$, B48L2P12 and B48L2K5P12. The dissipation factor of these compositions increases with the increasing of temperature due to the domain wall motion in the ferroelectric region. At the transition temperature the antiferroelectric phase starts taking place and reducing the domain wall. Consequently, above this temperature the dissipation factor continues diminishing as the amount of antiferroelectric phase increases. With K and La, a hump peak shifts toward lower temperature than the ones without either K or La. This result is similar to those from their dielectric permittivity data. Above the Curie point the conductivity dominates, resulting in an increase of the dissipation factor.

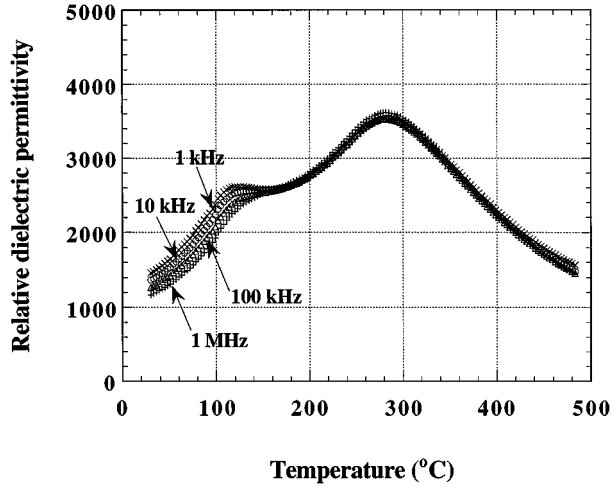

Figure 15 Change in the relative dielectric permittivity with temperature and frequency for 0.90($Bi_{0.45}La_{0.05}Na_{0.5}TiO_3$)-0.10$PbTiO_3$.

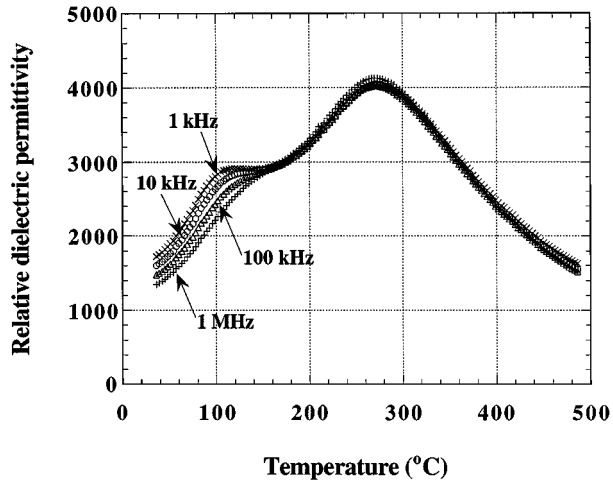

Figure 16 Change in the relative dielectric permittivity with temperature and frequency for 0.90($Bi_{0.45}La_{0.05}Na_{0.45}K_{0.05}TiO_3$)-0.10$PbTiO_3$.

Figs 15 and 16 also exhibit the similar effects of La and K on the dielectric properties of 0.90 ($Bi_{0.5}Na_{0.5}TiO_3$)-0.10$PbTiO_3$. La shifts both of the first transition and Curie point to lower temperatures, from 140°C [13] to 116°C and 323°C [13] to 280°C, respectively. It also decreases the maximum dielectric permittivity. K further extends the antiferroelectric range and increases the dielectric permittivity throughout the measuring temperatures. This effect is possibly related to the SEM microstructure of Figs 9 and 10 in which smaller grain size is a possible cause of higher dielectric permittivity at room temperature of this solid solution. The first phase transition, the Curie temperature and

TABLE I The first phase transition, Curie temperature and maximum dielectric permittivity at a frequency of 10 kHz for La- and K-doped-$Bi_{0.5}Na_{0.5}TiO_3$-$PbTiO_3$

Composition	First transition (°C)	Curie point (°C)	Max dielectric permittivity
12%Pb-doped $Bi_{0.5}Na_{0.5}TiO_3$	125	318	7100
B48L2P12	107	300	5400
B48L2K5P12	90	300	5950
B45L5P10	116	280	3530
B45L5K5P10	101	275	4040

the maximum value of dielectric permittivity at a frequency of 10 kHz for all these compositions are given in Table I. It should be noted that in this work the first phase transition temperature is determined from the intersection of tangent lines of the curves in the ferroelectric-antiferroelectric transition region and the Curie point is obtained from the temperature at the maximum dielectric permittivity.

4. Conclusions

12%Pb dopant develops long grains of $Bi_{0.5}Na_{0.5}TiO_3$. This effect can be reduced and the grain size decreases with the addition of La. In addition, La shifts the antiferroelectric region to lower temperature and decreases the maximum value of dielectric permittivity of 12%Pb-doped $Bi_{0.5}Na_{0.5}TiO_3$. In order to shift further lower the first phase transition closer to room temperature, K is a promising candidate dopant for $Bi_{0.5}Na_{0.5}TiO_3$-$PbTiO_3$ to enhance this performance. Unlike La, K raises the maximum dielectric permittivity and elongates the grain size of this solid solution.

Acknowledgment

This work was supported under the contract no. RSA5/2539 from the Thailand Research Fund and Chulalongkorn University.

References

1. G. A. SMOLENSKII, V. A. ISUPOV, A. I. AGRANOVSKAYA and N. N. KRAINIK, *Sov. Phys. Solid State* **2** (1961) 2651.
2. V. V. IVANOVA, A. G. KAPYSHEV, Y. N. VENEVTSEV and G. S. ZHDANOV, *Academy of Sciences USSR Bull., Phys. Series* **26** (1962) 358.
3. V. A. ISUPOV and T. V. KRUZINA, *ibid.* **47** (1983) 194.
4. I. P. PRONIN, P. P. SYRNIKOV, V. A. ISUPOV, V. M. EGOROV and N. V. ZAITSEVA, *Ferroelectrics* **25** (1980) 395.
5. K. SAKATA and Y. MASUDA, *ibid.* **7** (1974) 347.
6. J. SUCHANICZ, K. ROLEDER, A. KANIA and J. HANDEREK, *ibid.* **77** (1988) 107.
7. T. TAKENAKA and K. SAKATA, *ibid.* **95** (1989) 153.
8. T. TAKENAKA, K. SAKATA and K. TODA, *Jpn. J. Appl. Phys.* **28** (Suppl. 28-2) (1989) 59.
9. *Idem., Ferroelectrics* **106** (1990) 375.
10. T. TAKENAKA, K. MARUYAMA and K. SAKATA, *Jpn. J. Appl. Phys.* **30** (1991) 2236.
11. M. S. HAGIYEV, I. H. ISMAILZADE and A. K. ABIYEV, *Ferroelectrics* **56** (1984) 215.
12. M. S. GADZHIEV, A. K. ABIEV, V. A. ISUPOV and I. G. ISMAILZADE, *Sov. Phys. Solid State* **27** (1985) 1502.
13. S. KUHARUANGRONG and W. SCHULZE, *J. Amer. Ceram. Soc.* **79** (1996) 1273.
14. *Idem., ibid.* **78** (1995) 2274.

Received 24 January
and accepted 30 August 2000